JOURNAL OF GEOPHYSICAL RESEARCH, VOL. 93, NO. D5, PAGES 5213–5219, MAY 20, 1988

Effect of Computed Horizontal Diffusion Coefficients on Two-Dimensional N_2O Model Distributions

CHARLES H. JACKMAN

Atmospheric Chemistry and Dynamics Branch, NASA Goddard Space Flight Center, Greenbelt, Maryland

PAUL A. NEWMAN

Applied Research Corporation, Landover, Maryland

PAUL D. GUTHRIE AND MARK R. SCHOEBERL

Atmospheric Chemistry and Dynamics Branch, NASA Goddard Space Flight Center, Greenbelt, Maryland

The sensitivity of the N_2O distribution in our two-dimensional photochemical model to horizontal diffusion coefficients (both K_{yy} and K_{yz} values) has been explored. The residual circulation was computed using temperature data from the National Meteorological Center (NMC) and heating rates from Rosenfield et al. (1987). The K_{yy} and K_{yz} values were computed from these same data using quasi-geostrophic potential vorticity. For comparison we also computed self-consistent K_{yy} values from our residual circulation. The use of either set of these diffusion coefficients produced substantial changes in the N_2O distribution, especially in the middle to upper stratosphere and at high latitudes in the winter. In general, the changes lead to an enhanced transport of N_2O to higher latitudes with the set of self-consistent K_{yy} values transporting the greatest amount of N_2O. The enhanced transport increases the lifetime of N_2O because the photochemical lifetime is larger at high latitudes.

1. INTRODUCTION

One difficult aspect of two-dimensional modeling is that of prescribing the zonal mean transport and the diffusion of the atmosphere in a realistic way. In recent years, most two-dimensional models have been formulated using either a diabatic or a residual circulation as a zonal mean transport [*Miller et al.*, 1981; *Garcia and Solomon*, 1983; *Guthrie et al.*, 1984; *Ko et al.*, 1985; *Stordal et al.*, 1985]. A problem with these recent two-dimensional models is the inconsistency of a small diffusion field with a large zonal mean transport. *Newman et al.* [1986, this issue] and *Plumb and Mahlman* [1987] point out that this inconsistency implies a serious imbalance in the zonal momentum equation. For steady flow an approximate balance exists between the residual circulation's Coriolis torque and the flux of quasi-geostrophic potential vorticity (QPV). This flux can be calculated from the product of the diffusion coefficient (K_{yy}) and the zonal mean meridional gradient of QPV. If the specified diffusion is too small, then the flux of QPV will be too small to balance the residual circulation's Coriolis force. Most of the recently developed two-dimensional models specify small diffusion, at least in the stratosphere. For example, our two-dimensional model [see *Guthrie et al.*, 1984] had K_{yy} values similar in magnitude to those derived by *Kida* [1983] (i.e., 2×10^9 cm^2 s^{-1}).

Recently, *Newman et al.* [1986, this issue] derived diffusion coefficients, K_{yy} and K_{yz}, using QPV from NMC data. They showed that K_{yy} values are small for much of the year and much of the spatial domain of two-dimensional models, but that at certain times of the year, especially during winter in the high latitudes, very large K_{yy} values are possible. As part of this study, we will investigate the effects of these computed K_{yy} values and associated K_{yz} values on the tracer N_2O. For small QPV dissipation (generally true in the stratosphere), the QPV-derived Ks provide a good estimate of neutral diffusion [*Newman et al.*, this issue]. Hence the QPV-derived K_{yy} and K_{yz} can be used for N_2O, since it is largely a conservative stratospheric tracer. We, also, will investigate the effects of self-consistently calculated K_{yy} values, i.e., K_{yy}s computed directly from the residual circulation, on the tracer N_2O.

This paper is divided into seven sections. Separate model run cases are discussed in sections 2, 3, 4, and 5. In case 1 (section 2) we analyze the effects of the residual circulation alone on the N_2O distribution, which is not under strong photochemical control. Throughout the paper we will refer to case 1 as the base case. Case 2 (section 3) includes the K_{yy} of *Newman et al.* [this issue] with the residual circulation. Case 3 (section 4) includes both the K_{yy} and K_{yz} of *Newman et al.* [this issue] with the residual circulation. The self-consistent K_{yy}s will be included in case 4 (section 5). In each section we will compare and contrast the separate model cases. We will discuss how model results compare to experimental data in section 6. Finally, we will speculate on the effect of these K_{yy} and K_{yz} values on other trace gas distributions in our conclusions (section 7).

2. BASE CASE N_2O DISTRIBUTION: RESIDUAL CIRCULATION

We have used the two-dimensional model of *Guthrie et al.* [1984] modified somewhat for this study. For the base case model computation, we used the residual circulation computed from the use of heating rates of *Rosenfield et al.* [1987] with NMC monthly averaged temperature. We have com-

Paper number 8D0107.
0148-0227/88/008D-0107$05.00

TABLE 1. Reactions and Their Rates

Reaction	Rate
$N_2O + h\nu \rightarrow N_2 + O(^1D)$	$J_1 < 240$ nm
$O_3 + h\nu \rightarrow O_2 + O(^1D)$[a]	$J_2 < 310$ nm
$N_2O + O(^1D) \rightarrow NO + NO$	$k_3 = 6.7(-11)$[b]
$N_2O + O(^1D) \rightarrow N_2 + O_2$	$k_4 = 4.9(-11)$
$O(^1D) + N_2 \rightarrow O + N_2$	$k_5 = 1.8(-11)\exp(107/T)$
$O(^1D) + O_2 \rightarrow O + O_2$	$k_6 = 3.2(-11)\exp(67/T)$
$O(^1D) + N_2 + M \rightarrow N_2O + M$	k_7 [see *DeMore et al.*, 1985]

Rates correspond to those recommended by *DeMore et al.* [1985]. Units for photolysis processes are per second, binary reactions are cubic centimeters per second, and tertiary reactions are stated in $cm^6\ s^{-1}$.

[a]Spin conservation is not violated. $O_2(^1\Delta)$ is assumed to quench to O_2 rapidly.

[b]Read 6.7(−11) as 6.7×10^{-11}, etc.

puted photolysis rates and have included the effects of scattering of photons in all calculations utilizing the two-stream radiative transfer method discussed by *Herman* [1979], which is based on the matrix operator method of *Plass et al.* [1973]. The reactions and their rate coefficients used in our model computations are given in Table 1.

This particular computation, like those described by *Guthrie et al.* [1984] and *Jackman et al.* [1987], uses an ozone distribution specific to Nimbus 7 SBUV data [*McPeters et al.*, 1984], updated monthly. The O_2 number density also varies monthly because of the monthly NMC temperature changes affecting the total number density (M) of the atmosphere, and O_2 is tied to a mixing ratio of 0.21 over the entire altitude domain from the ground up to about 60 km. Only the species O_2 and O_3 are thought to significantly affect the background ultraviolet flux. Since both of these species are tied to observations, the calculated local ultraviolet flux should be a good approximation to that of the real atmosphere.

The residual transport streamlines are shown in Figure 1 for the month of January. This circulation pattern shows upward motion in the equatorial and low-latitude region, offset from the equator toward the southern hemisphere (commensurate with the solar zenith angle). The air motion bifurcates in the lower stratosphere into southward and northward motions. In the middle to high stratosphere, the pattern is simply a large cell with upward flow from −90° to −30°S, northward flow from about −30°S to 40°N, and poleward and downward flow from 40° to 90°N.

We show the trace gas N_2O in Figure 2 for the month of January for this base case model experiment (case 1). A mixing ratio boundary condition was imposed on N_2O at the ground to be 300 parts per billion by volume (ppbv) at all latitudes and times. This N_2O boundary condition was used in all model experiments. The stratospheric K_{yy} values used in case 1 are relatively low, increasing slightly into the troposphere, as shown in Figure 3. We have no seasonal variation in the diffusion field and assume that the symmetric parts of the diffusion tensor, K_{yy} and K_{zz}, are set to 2×10^9 $cm^2\ s^{-1}$ and 2×10^3 $cm^2\ s^{-1}$, respectively, everywhere above the tropopause. The off-diagonal parts of the diffusion tensor (K_{yz} and K_{zy}) are zero everywhere.

All model experiments were for 10 years of model time. This was a sufficient amount of model time for a seasonal cycle to repeat itself from one year to the next. The model study cases shown in this paper were all compared in the last year of their runs. The only computed species in the model experiments were N_2O and $O(^1D)$. The other species which are included in these model studies are NO, O, O_3, O_2, N_2, and M. Both NO and O are dummy species and therefore are not calculated. The other four species are not allowed to vary during the month but do change monthly. The list of reactions and their rates are given in Table 1.

The base case N_2O distribution shown in Figure 2 is dominated by the residual circulation pattern, at least in the stratosphere. The ballooning or bubblelike feature at low latitudes results from the direct circulation of the troposphere and lower to middle stratosphere. Anvillike features are apparent in the upper stratosphere of the northern hemisphere resulting from vertical shear in the meridional residual circulation.

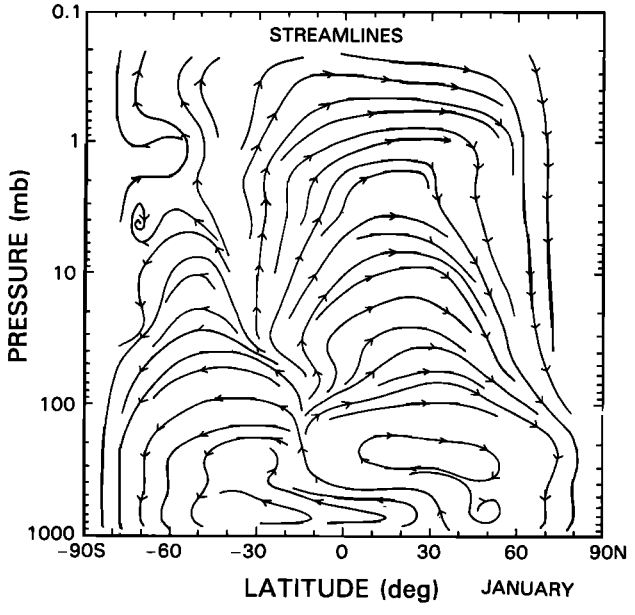

Fig. 1. Streamlines showing residual circulation wind patterns in our two-dimensional model for the month of January.

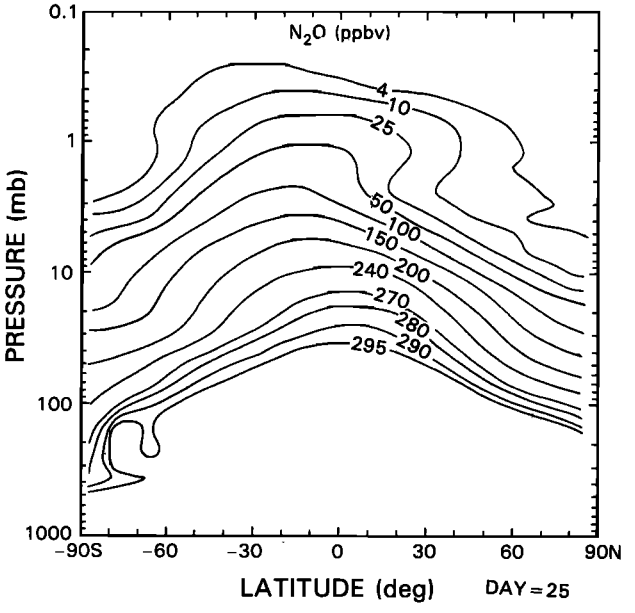

Fig. 2. Computed N_2O distribution for the base case model experiment on January 25.

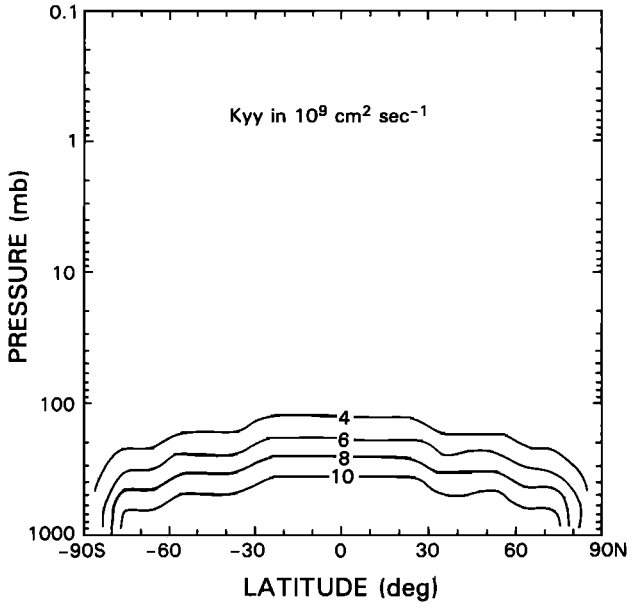

Fig. 3. Distribution of diffusion K_{yy} for the base case model experiment.

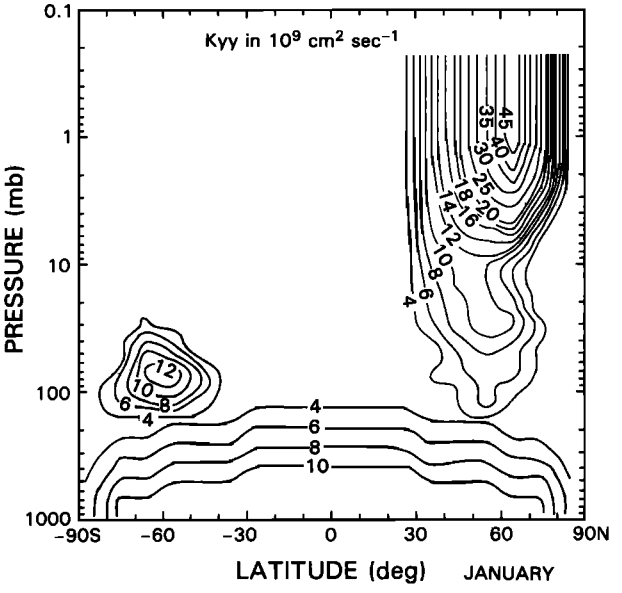

Fig. 4. Large computed diffusion K_{yy} for the month of January.

3. Effect of Computed K_{yy} Values on N_2O

Case 2 includes the K_{yy} values of *Newman et al.* [this issue] without K_{yz}. Setting $K_{yz} = K_{zy} = 0$ assumes that potential temperature is coincident with the pressure surfaces, which is not normally the case. We do not change the vertical diffusion K_{zz} values in any of our model computations. This experiment is performed mainly to indicate the sensitivity of N_2O to K_{yy} values that have a seasonal, latitude, and altitude dependence.

The K_{yy} values are expressed as the flux gradient ratio of the quasi-geostrophic potential vorticity field, where

$$K_{yy} = -\overline{(v'q')}/\bar{q}_y$$

where v' is the deviation from the zonal mean of the meridional velocity, q' is the deviation from the zonal mean of the potential vorticity, and $\bar{q}_y = \partial\bar{q}/\partial y$ is the zonal mean potential vorticity gradient (see *Newman et al.* [this issue] for a complete description of the K_{yy} computations).

At various places and times, K_{yy} values are negative. The negative values imply countergradient potential vorticity transport which can probably only occur under unusual circumstances [see *Newman et al.*, this issue]. We regard the negative K_{yy} values as unphysical. Furthermore, the N_2O distribution is perturbed in an extreme way by negative K_{yy} values. Thus we do not allow the K_{yy} values to be any smaller than 2×10^9 cm^2 s^{-1}.

Newman et al. [this issue] compute their values seasonally. We change our K_{yy} values monthly, linearly interpolating between seasons. The January K_{yy} field is shown in Figure 4.

Large values of K_{yy} (exceeding 4×10^{10} cm^2 s^{-1}) occur in the wintertime at high latitudes, especially in the northern hemisphere. The NMC temperature data goes up to 0.4 mbar; however, above 1 mbar the data is fairly uncertain. Therefore above the height of 1 mbar, we set the values of K_{yy} equal to those at 1 mbar. Our model extends to 0.23 mbar, thus we need to use CIRA 1972 temperature data above 0.4 mbar [see *Rosenfield et al.*, 1987]. These adjustments do not have an impact on the conclusions of this study.

Figure 5 compares case 1 N_2O (residual circulation and low K_{yy} and K_{zz} values) to case 2, with the computed K_{yy} values, for the day January 25 of both runs. We compare the two cases at a day in January because this is the month in which the maximum differences arise. Case 1 is illustrated by the solid lines, while case 2 (computed K_{yy} values) is illustrated by the dashed lines. In general, the larger horizontal diffusion, K_{yy}, has reduced concentrations of N_2O at middle to low latitudes and increased concentrations of N_2O at middle to high latitudes.

This is more easily illustrated in Figure 6, where the N_2O percentage change of case 2 from case 1 is plotted. Negative

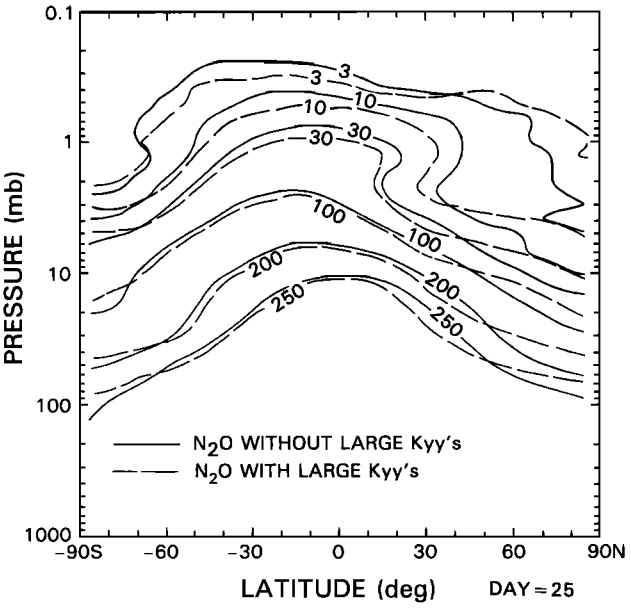

Fig. 5. Computed N_2O distributions from the base case model experiment (solid lines) and from the model experiment with the addition of the large computed K_{yy} values (dashed lines).

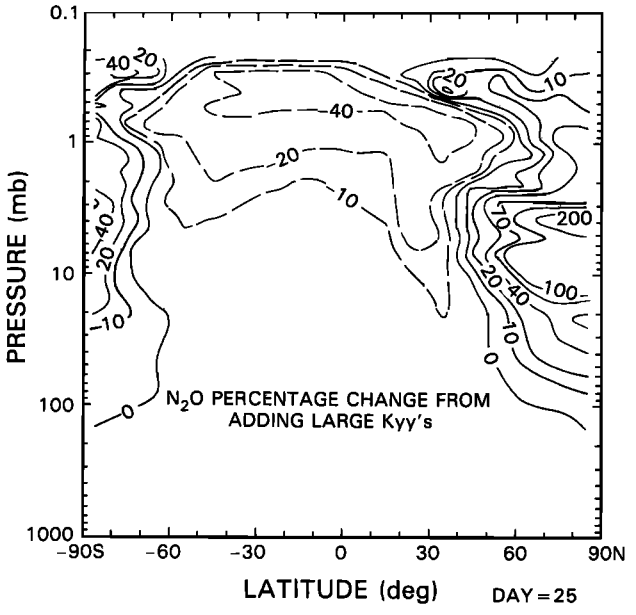

Fig. 6. Percentage change in the N_2O distribution from the base case model experiment to the model experiment which has the addition of the large computed K_{yy} values. Dashed lines show negative values, and solid lines show positive values.

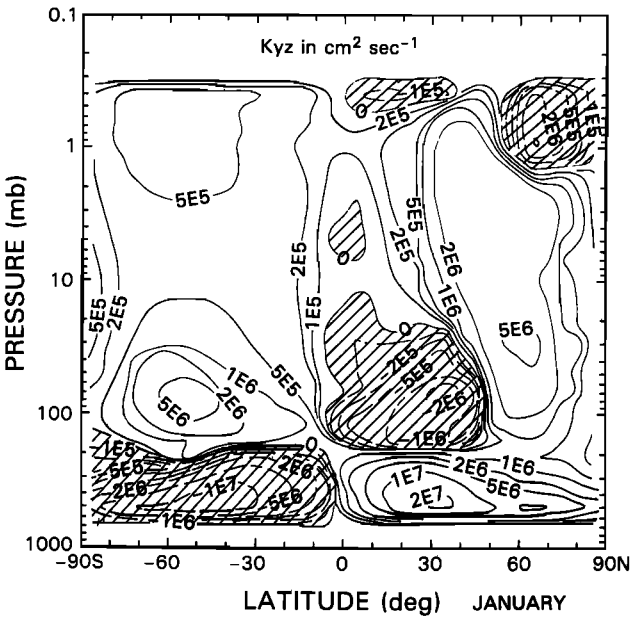

Fig. 7. Computed diffusion K_{yz} for the month of January. Dashed lines in cross-hatched areas show negative values, and solid lines show positive values.

values (decreases) are illustrated by dashed contour lines, and positive contours (increases) are solid lines. N_2O is decreased at middle to low latitudes by over 40% in some locations and is increased at middle to high latitudes, especially in the winter hemisphere. The largest contour plotted is a +200% contour. Clearly, as might be expected, the larger diffusion of case 2 has transported significant amounts of N_2O from the lower-latitude region to the higher-latitude region, especially in the middle to upper stratosphere and the lower mesosphere.

4. Effect of Computed K_{yz} Values on N_2O

In case 3 we include the off-diagonal components of the 2 × 2 diffusion matrix. These K_{yz} and K_{zy} values can be calculated using the potential temperature gradient and the K_{yy} distribution (lower limit of 2×10^9 cm^2 s^{-1} for K_{yy}), according to the relationship

$$K_{yz} = K_{zy} = -K_{yy}\,\overline{\Theta}_y/\overline{\Theta}_z$$

with $\overline{\Theta}_y = \partial\bar{\Theta}/\partial y$ and $\overline{\Theta}_z = \partial\bar{\Theta}/\partial z$, and where Θ is the potential temperature. This equation simply relates the mixing on isentropic surfaces to the mixing on pressure surfaces [*Newman et al.*, 1986].

We show the K_{yz} distribution for January in Figure 7. Values in the stratosphere range from above $+5 \times 10^6$ to below -2×10^6 cm^2 s^{-1}. Negative K_{yy} values have not been allowed in these model runs, but negative K_{yz} values are allowed. These negative K_{yz} values are related to poleward and downward mixing along zonal mean isentropes.

The percentage change of case 3 (computed K_{yz} and K_{yy}) from case 2 (computed K_{yy} alone) is given in Figure 8, again for January 25 of both cases. Concentrations of N_2O are reduced in the southern hemisphere at the higher latitudes and increased in the northern hemisphere at the higher latitudes. Both the K_{yy} and K_{yz} diffusion act to push N_2O into the winter higher-latitude region. This summer hemisphere decrease and winter hemisphere increase results from the upward tilt of the potential temperature surfaces from the summer to the winter poles.

Figure 9 compares the N_2O from the base case (case 1) with the case 3 (the computed K_{yy} and K_{yz} values). The additional diffusion has acted to smooth out the latitudinal gradients in the N_2O concentrations. Case 3 illustrates that most of the N_2O changes result from the larger K_{yy}, and that K_{yz} has a relatively smaller effect.

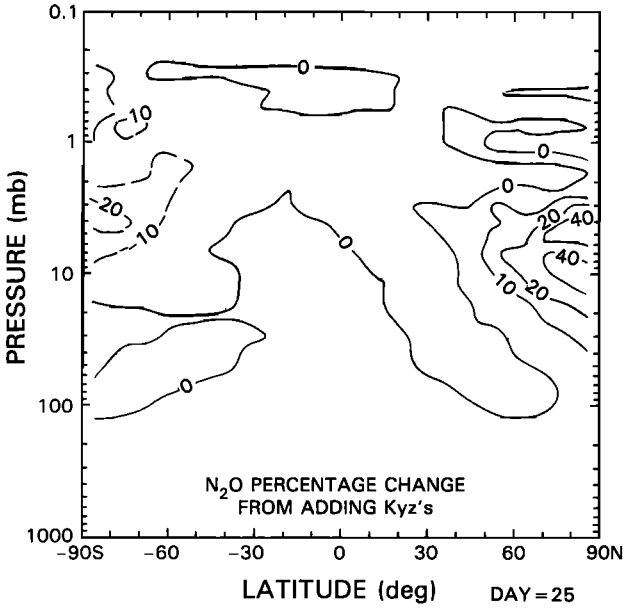

Fig. 8. Percentage change in the N_2O distribution from the model experiment with the large computed K_{yy} values to the model experiment which has both the large computed K_{yy} and K_{yz} values. Dashed lines show negative values, and solid lines show positive values.

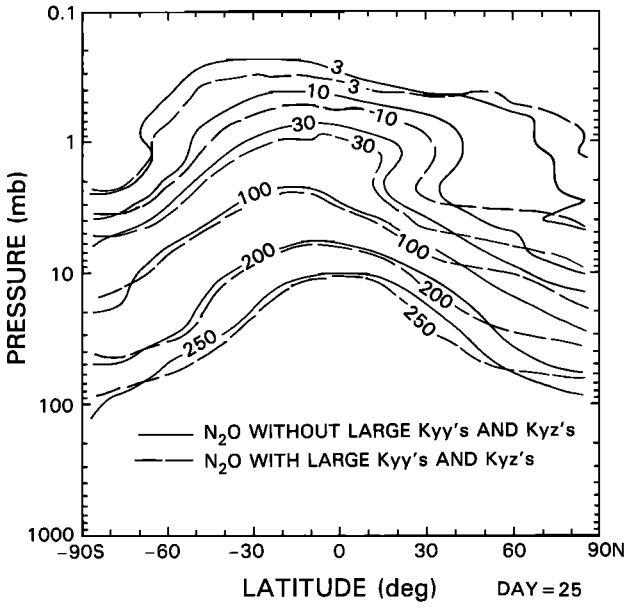

Fig. 9. Computed N_2O distributions from the base case model experiment (solid lines) and from the model experiment with the addition of both the large computed K_{yy} and K_{yz} values (dashed lines).

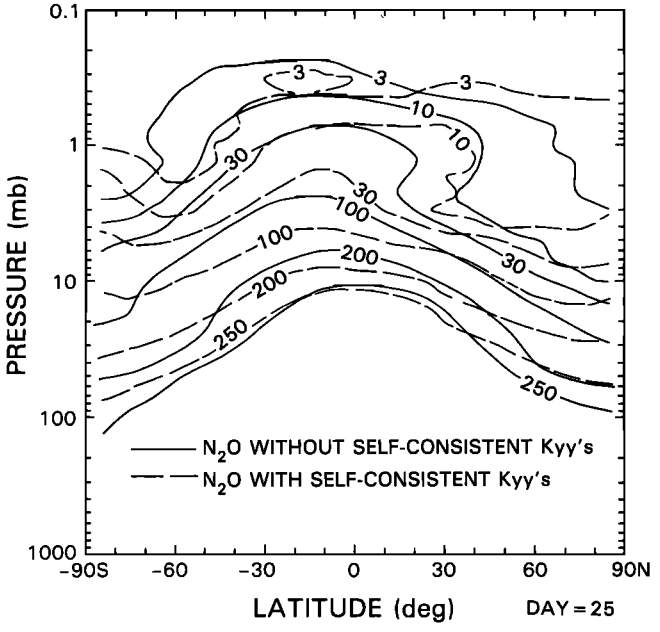

Fig. 10. Computed N_2O distributions from the base case model experiment (solid lines) and from the model experiment with the addition of the large self-consistent K_{yy} values (dashed lines).

5. Effect of Self-Consistent K_{yy} Values on N_2O

For case 4 we compute the K_{yy} values from our residual circulation. We can compute K_{yy} from the transformed zonal mean momentum equation (see *Newman et al.* [this issue] section 4.5). If we assume that the flow is steady, then most sources of momentum are small and K_{yy} can be computed from

$$K_{yy} = f\bar{v}^*/\overline{q_y}$$

where $f = 2\ \Omega \sin \phi$, $\Omega = 2\pi/86{,}400$ rad s^{-1}, ϕ is the latitude, and $\bar{v}^*$ = residual zonal mean meridional velocity. If we further assume that $\overline{q_y} \sim 4\ \Omega \cos \phi/a$ in the stratosphere [*Matsuno*, 1970], where a is the radius of the Earth, then we can write

$$K_{yy} \simeq a \tan \phi\ \bar{v}^*/2$$

With this simple relation we can compute K_{yy} values for our entire model grid which are consistent with our residual circulation. As in case 2, we find certain places where the K_{yy} values are negative (see, also, *Newman et al.* [this issue] Figures 16 and 17). We do not allow the negative values because we believe that they are unphysical (see discussion in section 3 on this point) and set the lowest value for K_{yy} to 2×10^9 cm^2 s^{-1}. Values of $\bar{v}^*$ range from about 10–100 cm s^{-1} and values of K_{yy} range from about 2–15 $\times$ 10^9 cm^2 s^{-1} in the stratosphere. The largest values of K_{yy} are about 7×10^{10} cm^2 s^{-1} and are located in the lower mesosphere at mid-latitudes.

Figure 10 compares case 1 N_2O (residual circulation and low K_{yy} and K_{zz} values) to this case with the self-consistent K_{yy} values, for January 25 of both runs. Case 1 is illustrated by the solid lines, while case 4 (self-consistent K_{yy} values) is illustrated by the dashed lines. In general, the self-consistent horizontal diffusion, K_{yy}, has reduced concentrations of N_2O at middle to low latitudes and increased concentrations of N_2O at middle to high latitudes.

This is also illustrated in Figure 11, where the N_2O percentage change of case 4 from case 1 is plotted. Negative values (decreases) are illustrated by dashed contour lines, and positive contours (increases) are solid lines. N_2O is decreased at middle to low latitudes by over 70% in some locations and is increased at middle to high latitudes, especially in the winter hemisphere. The largest contour plotted is a +200% contour. Large changes in the southern hemisphere mid-latitudes and polar region at 2 mbar result from the strong vertical gradients of the meridional residual circulation and, consequently, the K_{yy}. These excessive changes are due to small-scale details of the residual circulation (see Figure 1), and should not be considered as real. Nevertheless, as in case 2, the larger diffu-

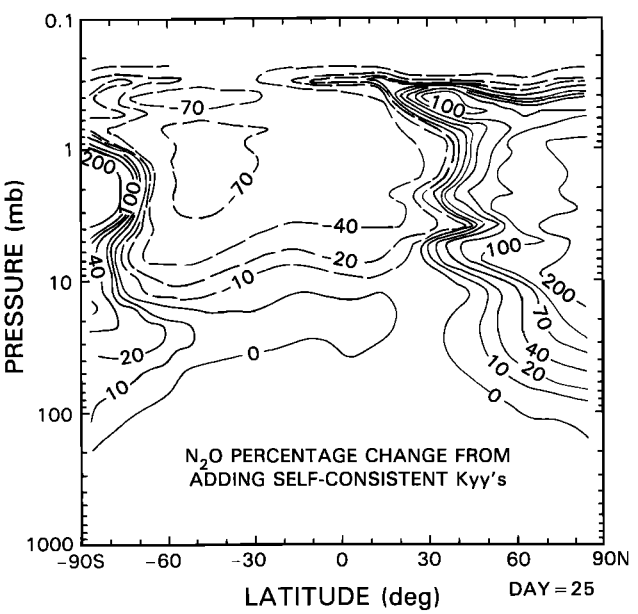

Fig. 11. Percentage change in the N_2O distribution from the base case model experiment to the model experiment which has the addition of the large self-consistent K_{yy} values. Dashed lines show negative values, and solid lines show positive values.

sion of case 4 has transported significant amounts of N_2O from the lower-latitude region to the higher-latitude region, especially in the middle to upper stratosphere and the lower mesosphere.

6. Discussion

Measurements of N_2O have been made through balloon measurements [*World Meteorological Organization (WMO)*, 1986], but the only set of measurements which are global in extent and the result of only one instrument's observations are the Stratospheric and Mesospheric Sounder (SAMS) measurements. In Figure 12 we overlay the N_2O model results (illustrated in Figures 9 and 10) with the January 1979 SAMS data adopted from *Jones and Pyle* [1984], which is generally similar to the 3-year SAMS average given by *Jones* [1984]. The N_2O from SAMS has a weak latitudinal gradient, indicative of larger mixing. The model results from the computed K_{yy} and K_{yz} values are larger in the low latitudes and smaller at the higher latitudes, especially in the middle to upper stratosphere. The self-consistent K_{yy} values give N_2O model results that are more similar to SAMS measurements, especially in the middle stratosphere. This may indicate either that the QPV-computed K_{yy} and K_{yz} values are too small, that the K_{zz} values are too small, that the advection fields (mainly our vertical velocities) are too large, or that a combination of all effects exists. Small-scale features of the residual circulation used here tend to produce detailed structures in the N_2O which are not observed in SAMS data.

The lifetimes from these four cases are shown in Table 2. In general, there was not much change, but there was an increase in the lifetime for case 2 (computed K_{yy}), case 3 (computed K_{yy} and K_{yz}), and case 4 (self-consistent K_{yy}). The higher lifetimes of N_2O in cases 2–4 resulted from its transport to the higher latitudes, where the photolysis rates are smaller.

We performed two other model experiments. In one experiment we set the K_{yy} values to 3×10^{10} cm^2 s^{-1} and $K_{yz} = K_{zy} = 0$ everywhere. Our results were similar to those presented by *Solomon et al.* [1986], which included a comparable study. The resulting N_2O distribution showed an overly flattened equator-to-pole mixing ratio surface slope, when compared to SAMS data. The lifetime of N_2O from this experiment was 236 years. Clearly, seasonal-, latitude-, and altitude-dependent K_{yy} values based on QPV are more realistic than merely increasing the K_{yy} values universally. In a second experiment we set the lowest K_{yy} values allowed to 1×10^8 cm^2 s^{-1}, rather than the 2×10^9 cm^2 s^{-1} described earlier, and found only minor changes in the resulting N_2O distributions.

The effect of advective transport uncertainties, due to the particular temperatures and heating rates used, was studied in another paper (P. D. Guthrie, C. H. Jackson, T. L. Kucsera, and J. E. Rosenfield, On the sensitivity of residual circulation models to temperature data, submitted to the *Journal of Geophysical Research*, 1988, hereafter referred to as Guthrie et al., submitted manuscript, 1988). In general, the addition of the computed K_{yy} and K_{yz} values to the model affected the total transport results less than a change in the temperature from NMC to LIMS data (compared by Guthrie et al., submitted manuscript, 1988), however, the addition of self-consistent K_{yy} values to the model affected the transport results as much as a change in temperature.

7. Conclusions: Implications

The N_2O distribution changed significantly when computed K_{yy} and K_{yz} values were added. In particular, the N_2O was transported from lower to higher latitudes. We find fairly large changes at high latitudes during winter. The lifetime of N_2O was increased a few percent by the addition of these computed diffusion fields. Use of self-consistently calculated K_{yy} values

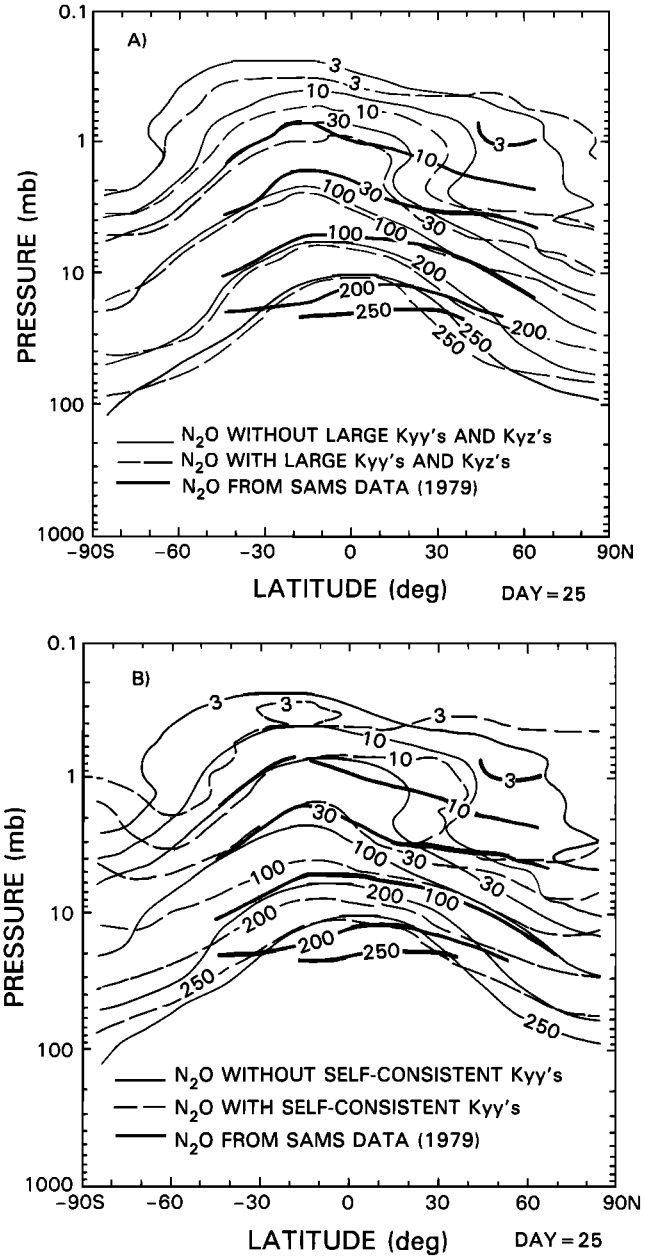

Fig. 12. Overlay of SAMS January measurements [*Jones and Pyle*, 1984] onto Figures 9 and 10 to show comparison of model and measurements. Computed N_2O distributions from the base case model experiment are indicated by the solid lines and the SAMS measurements are indicated by the heavy solid lines. (*a*) The model experiment showing the addition of both the large computed K_{yy} and K_{yz} values is indicated by the dashed lines, and (*b*) model experiment showing the addition of the large self-consistent K_{yy} values is indicated by the dashed lines.

TABLE 2. N_2O Lifetimes

Model Run	Lifetime, years
Case 1: Residual circulation (RC)	120
Case 2: RC plus computed K_{yy}	126
Case 3: RC plus computed K_{yy} and K_{yz}	127
Case 4: RC plus self-consistent K_{yy}	134

in the model leads to even larger transport of N_2O to high latitudes, with an even longer lifetime for N_2O.

Trace gases with sources at the ground and destruction at higher altitudes, especially in the stratosphere, will be influenced in a similar manner by the addition of more realistic diffusion fields. These gases include CH_4, $CFCl_3$, CF_2Cl_2, CH_3Cl, and CCl_4, which impact the NO_x, HO_x, and Cl_x radical distributions and therefore ozone. Changes in the two-dimensional distributions of several gases, which are important in the budget of ozone, probably will have an impact on assessment studies of chlorine and other atmospheric perturbations on the distribution of ozone. We plan on investigating this influence in a future model study.

Acknowledgments. The authors thank the two reviewers for constructive comments on the paper.

REFERENCES

DeMore, W. B., J. J. Margitan, M. J. Molina, R. T. Watson, D. M. Golden, R. F. Hampson, M. J. Kurylo, C. J. Howard, and A. R. Ravishankara, Chemical kinetics and photochemical data for use in stratospheric modeling, *JPL Publ., 85-37*, 1985.

Garcia, R. R., and S. Solomon, A numerical model of the zonally averaged dynamical and chemical structure of the middle atmosphere, *J. Geophys. Res., 88*, 1379–1400, 1983.

Guthrie, P. D., C. H. Jackman, J. R. Herman, and C. J. McQuillan, A diabatic circulation experiment in two-dimensional photochemical model, *J. Geophys. Res., 89*, 9589–9602, 1984.

Herman, J. R., The response of stratospheric constituents to a solar eclipse, sunrise, and sunset, *J. Geophys. Res., 84*, 3701–3710, 1979.

Kida, H., General circulation of air parcels and transport in the stratosphere and troposphere derived from CCM, 1, Mean mass flow in the lower stratosphere, *J. Meteorol. Soc. Jpn., 61*, 171–186, 1983.

Jackman, C. H., P. D. Guthrie, and J. A. Kaye, An intercomparison of nitrogen-containing species in Nimbus 7 LIMS and SAMS data, *J. Geophys. Res., 92*, 995–1008, 1987.

Jones, R. L., Satellite measurements of atmospheric composition: Three years' observations of CH_4 and N_2O, *Adv. Space Res., 4*, 121–130, 1984.

Jones, R. L., and J. A. Pyle, Observations of CH_4 and N_2O by the Nimbus 7 SAMS: A comparison with in situ data and two-dimensional numerical model calculations, *J. Geophys. Res., 89*, 5263–5279, 1984.

Ko, M. K. W., K. K. Tung, D. K. Weinstein, and N. D. Sze, A zonal-mean model of stratospheric tracer transport in isentropic coordinates: Numerical simulations for nitrous oxide and nitric acid, *J. Geophys. Res., 90*, 2313–2329, 1985.

Matsuno, T., Vertical propagation of stationary planetary waves in the winter northern hemisphere, *J. Atmos. Sci., 27*, 871–883, 1970.

McPeters, R. D., D. F. Heath, and P. K. Bhartia, Average ozone profiles for 1979 from the Nimbus 7 SBUV instrument, *J. Geophys. Res., 89*, 5199–5214, 1984.

Miller, C., D. L. Filkin, A. J. Owens, J. M. Steed, and J. P. Jesson, A two-dimensional model of stratospheric chemistry and transport, *J. Geophys. Res., 86*, 12,039–12,065, 1981.

Newman, P. A., M. R. Schoeberl, and R. A. Plumb, Horizontal mixing coefficients for two-dimensional chemical models calculated from National Meteorological Center data, *J. Geophys. Res., 91*, 7919–7924, 1986.

Newman, P. A., M. R. Schoeberl, R. A. Plumb, and J. E. Rosenfield, Mixing rates calculated from potential vorticity, *J. Geophys. Res.*, this issue.

Plass, G. N., G. W. Kattawar, and F. E. Catchings, Matrix operator theory of radiative transfer, 1, Rayleigh scattering, *Appl. Opt., 12*, 314–329, 1973.

Plumb, R. A., and J. D. Mahlman, The zonally averaged transport characteristics of the GFDL general circulation/transport model, *J. Atmos. Sci., 44*, 298–327, 1987.

Rosenfield, J. E., M. R. Schoeberl, and M. A. Geller, A computation of the stratospheric diabatic residual circulation using an accurate radiative transfer model, *J. Atmos. Sci., 44*, 859–876, 1987.

Solomon, S., J. T. Kiehl, R. R. Garcia, and W. Grose, Tracer transport by the diabatic circulation deduced from satellite observations, *J. Atmos. Sci., 43*, 1603-1617, 1986.

Stordal, F., I. S. A. Isaksen, and K. Horntveth, A diabatic circulation two-dimensional model with photochemistry: Simulations of ozone and ground released tracers, *J. Geophys. Res., 90*, 5757–5776, 1985.

World Meteorological Organization, Atmospheric ozone, 1985, *Rep. 16*, Global Ozone Res. and Monit. Proj., Geneva, Switzerland, 1986.

P. D. Guthrie, C. H. Jackman, and M. R. Schoeberl Atmospheric Chemistry and Dynamics Branch, Code 616, NASA Goddard Space Flight Center, Greenbelt, MD 20771.

P. A. Newman, Applied Research Corporation, 8201 Corporate Drive, Landover, MD 20785.

(Received July 30, 1987;
revised January 25, 1988;
accepted February 1, 1988.)